HHS Public Access

Author manuscript

Mol Cancer Res. Author manuscript; available in PMC 2018 August 01.

Published in final edited form as:

Mol Cancer Res. 2017 August ; 15(8): 1096–1105. doi:10.1158/1541-7786.MCR-16-0477.

Differential Expression of OATP1B3 Mediates Unconjugated Testosterone Influx

Tristan M. Sissung[1], **Ariel M. Ley**[2], **Jonathan D. Strope**[2], **Edel M. McCrea**[2], **Shaunna Beedie**[2], **Cody J. Peer**[1], **Suneet Shukla**[3], **Jennifer van Velkinburgh**[2], **Kelie Reece**[2], **Sarah Troutman**[2], **Tessa Campbell**[2], **Elena Fernandez**[2], **Phoebe Huang**[2], **Jordan Smith**[4], **Nilay Thakkar**[5], **David J. Venzon**[6], **Stefan Brenner**[7], **Wooin Lee**[8], **Maria Merino**[9], **Ji Luo**[4], **Walter Jager**[7], **Douglas K. Price**[2], **Cindy H. Chau**[2], and **William D. Figg**[1,2,*]

[1]Clinical Pharmacology Program, Office of the Clinical Director, National Cancer Institute, Bethesda, MD

[2]Molecular Pharmacology Section, Genitourinary Malignancies Branch, National Cancer Institute, Bethesda, MD

[3]Laboratory of Cell Biology, National Cancer Institute, Bethesda, MD

[4]Laboratory of Cancer Biology and Genetics, National Cancer Institute, Bethesda, MD

[5]Department of Pharmaceutical Sciences, College of Pharmacy, University of Kentucky, Lexington, Kentucky, USA

[6]Biostatistics and Data Management Section, National Cancer Institute, Bethesda, MD

[7]Department of Clinical Pharmacy and Diagnostics, University of Vienna, A-1090 Vienna, Austria

[8]College of Pharmacy, Seoul National University, Seoul, Korea

[9]Translational Surgical Pathology Section, National Cancer Institute, Bethesda, MD

Abstract

Castration resistant prostate cancer (CRPC) has greater intratumoral testosterone concentrations than similar tumors from eugonadal men; simple diffusion does not account for this observation. The present study was undertaken to ascertain the androgen uptake kinetics, functional, and clinical relevance of de novo expression of the steroid hormone transporter OATP1B3 (SLCO1B3). Experiments testing the cellular uptake of androgens suggest that testosterone is an excellent substrate of OATP1B3 (KM=23.2μM; VMAX=321.6pmol/mg/min), and cells expressing a doxycycline-inducible SLCO1B3 construct had greater uptake of a clinically relevant concentration of 3H-testosterone (50nM; 1.6-fold, P=0.0027). When compared to Slco1b2 (−/−) mice, Slco1b2 (−/−)/hSLCO1B3 knockins had greater hepatic uptake (15% greater AUC, P=0.0040) and lower plasma exposure to 3H-testosterone (17% lower AUC, P=0.0030). Of 82 transporters genes, SLCO1B3 is the second-most differentially-expressed transporter in CRPC cell lines (116-fold vs androgen sensitive cells), with a differentially-spliced cancer-type ct-SLCO1B3

*Corresponding author: William D. Figg, PharmD, Clinical Pharmacology Program, National Cancer Institute, 9000 Rockville Pike, Building 10, Room 5A01, Bethesda, MD, 20892; Phone: (301) 402-3623; Fax: (301) 402-8606; wdfigg@helix.nih.gov.

The authors declare no potential conflicts of interest.

making up the majority of SLCO1B3 expression. Overexpression of SLCO1B3 in androgen responsive cells results in 1.5- to 2-fold greater testosterone uptake whereas siRNA knockdown of SLCO1B3 in CRPC cells did not change intracellular testosterone concentration. Primary human prostate tumors express SLCO1B3 to a greater extent than ct-SLCO1B3 (26% of total SLCO1B3 expression vs 0.08%), suggesting that androgen uptake in these tumor cells also is greater. Non-liver tumors do not differentially express SLCO1B3.

INTRODUCTION

Androgen deprivation therapy (ADT), or the suppression of gonadal androgens via surgical or medical castration, remains the mainstay of treatment for advanced and metastatic prostate cancer. Despite the efficacy of ADT, progression inevitably occurs with the emergence of a castration-resistant prostate cancer (CRPC) phenotype that has adapted to survive in a low androgen environment (1) and rely on persistent androgen receptor (AR) signaling in most cases (2). CRPC is defined as a progressive rise in prostate-specific antigen (PSA) despite castrate levels of testosterone (less than 50 ng/dL). While ADT effectively decreases serum testosterone by >90%, intraprostatic concentrations of androgen only decline by 75% in men with localized disease (3) whereas CRPC metastases have significantly elevated intratumoral testosterone levels compared to tumors in eugonadal men (4).

Recent advances in the treatment armamentarium of CRPC have focused on selective inhibition of pathways involved in persistent androgen production, AR signaling axis, and/or ligand-AR interaction. Since persistent AR signaling may arise from the presence of residual intraprostatic androgens, elucidating sources (e.g., *de novo* androgen biosynthesis) or mechanisms that modulate intracellular tissue androgens remain a key target for prostate cancer drug development. For years it has been postulated that maintenance of intratumoral androgen concentrations was the result of passive diffusion; however this process could not completely account for the intracellular testosterone uptake rate (5). Our laboratory was the first to demonstrate that the organic anion polypeptide 1B3 (OATP1B3) transporter concentrates unconjugated testosterone in cells (Hamada et al, 2008). We further showed that OATP1B3 is expressed *de novo* in prostate tumor cells and that polymorphic variations in the *SLCO1B3* gene encoding OATP1B3 are related to clinical outcome in men with prostate cancer receiving ADT or those with CRPC (Hamada et al, 2001; Sharifi et al 2008). Subsequent studies have confirmed our findings supporting the role of steroid transporters in modulating intracellular androgen concentrations, thereby promoting CRPC progression (6,7).

OATP1B3 is abundantly expressed in human liver cells and expressed *de novo* in many types of cancer cells including prostate cancer (8). It is responsible for the uptake of numerous substrates into the liver (9), yet in spite of its tumoral expression, the uptake of OATP1B3 substrates into tumors is poorly characterized (10). Specifically, the precise kinetics of testosterone uptake have not yet been ascertained including whether these transporters are active in prostate cancer cells; therefore, it is unknown to what extent OATP1B3 expression contributes to testosterone uptake in prostate cancer. We hypothesize that OATP1B3 may be

a driver of resistance to ADT through the mechanism of increasing uptake of residual androgens into prostate tumors. The current study was undertaken to evaluate the kinetics of testosterone transport and its inhibition by a known OATP1B3 inhibitor as well as to establish the functional and clinical relevance of OATP1B3 expression in prostate cancer cell lines and tissues.

MATERIALS AND METHODS

Reagents

Tritiated testosterone, 4-androstene-3,17-dione (androstenedione) and 5-androstan-17-ol-3-one (DHT) were purchased from American Radiolabeled Chemicals (Saint Louis, MO). Tritiated methotrexate (MTX) was purchased from Perkin Elmer (Hanover, MD). Unlabeled testosterone, androstenedione and DHT as well as ursolic acid, L-proline, sodium butyrate, and Triton X-100 were purchased from Sigma-Aldrich (St. Louis, MO). Chetomin was purchased from Sigma-Aldrich (St. Louis, MO). Cell culture media and antibiotics were obtained from Invitrogen (Carlsbad, CA) unless stated otherwise.

Polyclonal EGFP antibody (ab111258) was purchased from ABCAM (Cambridge, MA), and monoclonal actin (C-2) antibody was purchased from Santa Cruz Biotechnology (Santa Cruz, CA). IRDye 800CW goat anti-mouse, IRDye 800CW donkey anti goat, and Odyssey blocking buffer were obtained from LI-COR (Lincoln, NE).

Cell lines and their maintenance

Chinese hamster ovary (CHO) cell lines stably expressing human OATP1B3 have been described (11,12). CHO wild type (CHO-WT) cells were transfected with the empty pcDNA5/FRT vector (CHO-pcDNA5/FRT) and were used as a control. Both cell lines were kindly provided by Dr. B. Stieger, Division of Clinical Pharmacology and Toxicology, University Hospital, Zurich, Switzerland. All prostate tumor cell lines (LNCaP, 22Rv1, PC3, DU145, and NE-1.8) were purchased from American Type Culture Collection (ATCC, Manassas, VA).

The OATP1B3-transfected CHO cells and CHO-WT cells were cultured in Dulbecco's Modified Eagle Medium (DMEM) containing 10% fetal bovine serum, 50 mM L-proline, 100 U/ml penicillin/streptomycin, and 500 μg/mL geneticin G-418. LNCaP and 22Rv1 cells were maintained in phenol red-free RPMI 1640 medium supplemented with 10% fetal bovine serum, 50 U/mL penicillin, and 50 mg/mL streptomycin unless otherwise indicated. PC3 cells were maintained in Ham's F12K medium and DU145 cells were maintained in Eagles Minimal Essential Medium (EMEM), both supplemented with 10% fetal bovine serum, 50U/mL penicillin, and 50mg/mL streptomycin unless otherwise indicated. Cells were incubated at 37°C in an atmosphere containing 5% CO_2 and 95% humidity. To mimic hypoxic conditions, cells were treated with the hypoxia mimetic, cobalt chloride (150 μM $CoCl_2$) (Sigma-Aldrich).

Transport of tritiated testosterone, 4-androstan-3,17-dione and 5-androstan-17-ol-3-one in stably transfected OATP1B3 CHO cells

Transport assays were performed as described (1). Briefly, cells were washed three times with 2 ml of pre-warmed (37 °C) uptake buffer (116.4 mM NaCl, 5.3 mM KCl, 1 mM NaH_2PO_4, 0.8 mM $MgSO_4$, 5.5 mM D-glucose and 20 mM HEPES, pH adjusted to 7.4 with Trizma base) and uptake was started by adding 1 mL of uptake buffer containing 2 μCi of the ^{3}H-labeled compounds and the initiated concentrations of unlabeled substrates in the presence or absence of ursolic acid.

After the initiated time period at 37°C, uptake was stopped by removing the uptake solution and washing the cells five times with 2 mL of ice-cold uptake buffer. The cells were then lysed with 1 mL of Triton X-100 (dissolved in PBS). A 500 mL aliquot was used for liquid scintillation counting. Protein concentrations were determined with the BCA assay (Pierce Science, Rockford, IL) using bovine serum albumin (BSA) as the standard.

Kinetic analysis for the uptake of ^{3}H-labeled testosterone, androstenedione, and DHT was performed for a 1–100 μM substrate concentration range. Cellular uptake rates were determined after normalizing for incubation time and total protein content. OATP1B3 net uptake rates were calculated as the difference in the uptake rate of the transporter and CHO-WT for each concentration. Kinetic parameters, Km and Vmax, were determined with non-linear regression analysis using the Michaelis-Menten equation. To further confirm the OATP1B3-mediated transport, uptake experiments of ^{3}H-labeled testosterone, androstenedione, and DHT (1 μM, respectively) were also performed in the presence and absence of the OATP1B3-inhibitor ursolic acid (1–100 μm). Assay conditions and incubation time were identical to those described above.

Doxycyline-inducible OATP1B3 expressing cell lines

EGFP-SLCO1B3 CDS DNA segment was purchased from Genewiz and cloned downstream of a tetracycline (TET)-response element into a pINDUCER plasmid between Age1 and Mlu1 restriction sites, as was previously published using the KRAS oncoprotein (13). Plasmids were packaged in HEK293T cells (ATCC) using Trans-IT reagent (Mirus, Madison, WI). Transduction of 22Rv1, LNCaP, DU145, and PC3 cells was accomplished with EGFP-SLCO1B3 virus in media containing 1 μg/mL polybrene. Transduced cells were plated on 6-well plates in cell type appropriate media. Cells were selected with 4 μg/mL puromycin for 3–4 days. Transduction was confirmed by imaging with fluorescence microscopy, quantitative PCR (qPCR), and Western blotting.

Pharmacokinetic profiles of ^{3}H-labeled testosterone in knockout and humanized mice

Pharmacokinetics were conducted using male FVB.129P2-Del(*Slco1b2-Slco1a5*)1Ahs (*Slco2b1* knockout) and male FVB.129P2-Del(*Slco1b2-Slco1a5*)1Ahs FVB.129P2-Del(*Slco1b2-Slco1a5*)1Ahs Tg(APOE-*SLCO1B3*)1Ahs (*Slco2b1* knockout/*hSLCO1B3* knockin) mice. All mice were administered a single bolus of ^{3}H-testosterone through the tail vein (0.3 μg/kg dissolved in normal saline) and the concentration of testosterone in the plasma and liver were determined at several timepoints: 2, 5, 10, 15, 30, 45, and 60 minutes (n=3–6 per timepoint). Plasma was collected by centrifuging heparinized whole blood

(obtained via cardiac puncture) at 900 x *g* for 5 minutes, and liver tissue was homogenized (BeadBug Benchtop Homogenizer, Benchmark Scientific, Edison, NJ). Standard curves were constructed for each of the tissue types, and the concentration within each sample type was determined by interpolation. Testosterone exposure in each tissue was determined by calculating AUC and tested by Bailer's method for destructive sampling (14). Approval for all experiments was granted by the NCI Animal Care and Use Committee, and all experiments were done in accordance with the NCI ACUC guidelines.

SLCO1B3 expression

Prostate cancer cells were cultured as described above and treated with vehicle control (1% DMSO), $CoCl_2$ (150 μM), chetomin (100 nM), or chetomin and $CoCl_2$. Total RNA extraction was performed using the QIAshredder and RNAeasy mini kit (Qiagen, Valencia, CA) according to the manufacturer's protocol. RNA concentration was determined using a NanoDrop spectrophotometer (Molecular Devices, Sunnyvale, CA). Purified RNA (0.24–0.32 μg) from prostate cancer cells was reverse transcribed per 30 μl cDNA synthesis reaction using the Superscript III First-Strand Synthesis System for RT-PCR (Invitrogen) according to the manufacturer's protocol. Detection of different SLCO1B3 transcripts were conducted using TaqMan assays (Life Technologies (Thermo), Grand Island, NY) per the manufacturer's instructions on a StepOnePlus Real-time PCR system (Applied Biosystems, Foster City, CA). Primers were designed using NM_019844.3, which includes 16 exons and a new exon 2 that was not previously included in the gene. Human normal and tumor tissue samples were obtained from Origene (TissueScan Cancer Survey Panel III, Rockville, MD). RNA was isolated from patients of mixed age, clinical diagnosis, and with various tumor stages and qPCR was conducted as above. The panel includes 384 samples encompassing 22 cancers and matched normal tissues. The number of samples corresponding to different tumor types and the number of samples derived from different tumor grades are reported in Table S1.

Western Blot Analysis

Cells were lysed with 300 μL ice-cold lysis buffer (2.5% (v/v) Tris pH 8, 3% (v/v) 5 M NaCl, 0.4% (v/v) 0.5 M EDTA, 1% (v/v) Triton-X 100, and complete protease inhibitors). After 30 minutes of incubation on ice, cell lysates were centrifuged at 7500 rpm for 10 minutes. Supernatants were collected and total protein concentration was determined using the BCA assay (Thermo Scientific, Waltham, MA) according to the manufacturer's protocol. Cell lysates were subjected to SDS-PAGE and analyzed by Western blotting with anti-EGFP antibody (Abcam, #ab6673), anti-actin monoclonal antibody (Santa Cruz Biotechnology, #sc-8432), and anti-Na+/K+ ATPase (Santa Cruz Biotechnology, #sc28800). Primary antibody was immunoreacted with fluorophore-conjugated goat anti-mouse IgG. Bound antibodies were visualized, and densitometry was completed via the Odyssey Infrared Imaging System and Odyssey software (LI-COR). Antibody dilutions were as follows: ABCAM goat pAB to EGFP antibody – 1:5000, and SCB mouse mAB to actin (C-2) antibody – 1:1000, G800 = IRDye 800CW donkey anti goat (incubated with ABCAM) 1: 15,000, M800 = IRDye 800CW goat anti-mouse (incubated with ACTIN) 1: 20,000. We were unable to detect membrane-bound OATP1B3 using several commercially available

antibodies, instead detecting non-specific bands in the cytoplasmic fraction that are approximately the same size of non-GFP-labeled OATP1B3 (~84kDa; Figure S1).

Testosterone uptake in prostate cell lines

Cells were grown overnight in maintenance media (MM). Maintenance media was then aspirated and replaced with chetomin (100 nM in 1% DMSO) treatment media (TM) (TM is same as MM, but 10% charcoal dextran stripped FBS was used and untreated media contained 1% DMSO). Cells were grown in TM for 24 hours (22Rv1) or 48 hours (LNCaP).

For transport experiments in prostate tumor cell lines, Hank's Balanced Salt Solution (HBSS; 10.0 mM HEPES) was obtained from Stemcell Technologies (Vancouver, Canada), and supplemented with additional HEPES (final concentration was 12.5 mM). For transport experiments, ~70% confluent cells were gently washed using warm Dulbecco's Phosphate Buffered Saline (DPBS), warm HBSS was added containing 50 nM unlabeled testosterone, cells were exposed for 1 hour, re-washed with DPBS, and exposed to ^{3}H-testosterone (50 nM) and/or ursolic acid (350 nM). To obviate confounding factors, such as rapid diffusion of testosterone into cells, binding of testosterone to cell culture plastic, and binding of testosterone to intracellular receptors, we then exposed cells to 1 hour of unlabeled testosterone (50nM), washed with fresh media and then treated with 50nM tritiated testosterone for 5, 10, 30, and 60 minutes. Similar experiments were conducted using methotrexate (5 μM) as a positive control.

TaqMan Low Density Arrays (TLDAs)

Expression levels of transporters were measured using custom-made TLDAs (Applied Biosystems) as described by Gillet et al. (Mol. Pharmaceutics, 2011, 8 (6), 2080–2088). Briefly, cDNA was prepared from total RNA isolated from LNCaP, 22Rv1, PC3, and DU145 cell lines. The cDNA was mixed with TaqMan Universal PCR Master Mix (Applied Biosystems) and the samples were loaded on the TLDA cards. The real-time PCR was run on an ABI Prism 7900 HT sequence detection system (Applied Biosystems, Foster City, CA, USA) as per the manufacturer's instructions. Data from TLDAs were collected in sequence detection system (SDS) files, and analyzed using relative quantification (RQ) Manager software. The rRNA 18s was used for quality control in four replicates. The median expression of each sample was subtracted from all gene expression data for that sample.

siRNA Transfection

Specific knockdown was achieved using siRNAs against *SLCO1B3* or Allstars negative control siRNA from Qiagen. Optimization of siRNA knockdown was completed in androgen-responsive prostate cancer cell lines (22Rv1 and LNCaP) and CRPC cell lines (Du145 and PC3). Cells were transiently transfected with control or *SLCO1B3* siRNA at 200nM using Lipofectamine 2000 (Invitrogen) according to the manufacturer's instructions for 24 hours.

The four commercially available siRNAs for *SLCO1B3* were tested in each cell line, gene expression of total-*SLCO1B3* was measured using semiquantitative real-time PCR, and siRNAs, were chosen based on knockdown efficiency: SI02643725 (FlexiTube siRNA)

targets sequence TAGCTATGCCTTTATGGTTAA SI02643718 (FlexiTube siRNA) targets sequence ATGGATAAGTCTATGCATCTA SI00124418 (FlexiTube siRNA) targets sequence TTCATCTATGTTGCAATTCAA SI00124411 (FlexiTube siRNA) targets sequence CTAGAATATAAGGGAGGTAAA

Data analysis

To ascertain statistical significance of the EMSA experiments, densitometry data were collected using ImageJ software using the original images (Rasband, W.S., ImageJ, U. S. National Institutes of Health, Bethesda, Maryland, USA, http://imagej.nih.gov/ij/, 1997–2015), standardized to untreated control, and transformed by taking the square root of each value. Finally, values were fitted to a linear model as a function of log(unlabeled probe concentration) and F-tests were conducted to determine if the wild-type probes inhibited HIF-binding differently from mutant probes. IC50 and kinetic parameters were calculated using non-linear regression analysis in GraphPad Prism (GraphPad Software, San Diego, CA). Induced androgen and protein concentrations and t-SLCO1B3, lt-SLCO1B3, and ct-SLCO1B3 expression were tested by analysis of variance or t-tests when agreement with normality assumptions was observed or by Wilcoxon rank sum tests, with stratification by experiment when needed. Fisher's exact tests were applied to comparisons of proportions. Expression of lt-SLCO1B3 and ct-SLCO1B3 relative to t-SLCO1B3 was analyzed using a left-censored logistic model after logarithmic data transformation. All p values are two-tailed and are not corrected for multiple comparisons in this broad exploratory investigation.

RESULTS

Kinetics of androgen transport by OATP1B3

To characterize OATP1B3-mediated androgen transport, we determined the uptake kinetics of ^{3}H-labeled testosterone and two steroid hormones that are structurally similar to testosterone, tritiated androstenedione (4-androsten-3,17-dione), and the DHT precursor, 5′-adione (5-androstane-17-ol-3-one; DHT) (15). Each of these hormones showed a limited, but significant, active uptake into CHO cells stably transfected with OATP1B3 versus those transfected with vector control (Figure 1A–C). Of these, testosterone had the highest affinity for the transporter (K_m = 23.2± 3.9 μM, V_{max} 321.6± 16.5 pmol/mg/min) compared to [^{3}H]-4-androstan-3,17-dione (androstenedione; K_m = 31.7± 9.5 μM, V_{max} 109.9± 13.7 pmol/mg/min) and [^{3}H]-5-androstan-17-ol-3-one (DHT; K_m = 30.4± 9.3 μM, V_{max} 102.8± 13.1 pmol/mg/min).

Next, we assessed whether OATP1B3-mediated androgen uptake could be inhibited by ursolic acid, a specific and selective inhibitor of OATP1B3 that inhibited fluorescent methotrexate uptake (IC_{50}=2.3μM) (16). As shown in Figure 1A–C, the uptake of all steroid hormones was inhibited by ursolic acid. Surprisingly, the IC_{50} of testosterone and androstenedione uptake was ~60–75 times lower than that of fluorescent methotrexate (0.030± 0.0018 μM, 0.038± 0.0057 μM), and the IC_{50} of DHT was ~5 times lower (0.45± 0.16 μM). Therefore, ursolic acid may be a better inhibitor of steroid hormone uptake than it is for other substrates of OATP1B3.

To confirm that testosterone is transported by OAT1B3 in prostate cancer cells, we developed stable prostate cancer cells using a doxycycline (DOX)-inducible gene expression system to regulate expression of GFP-labeled OATP1B3 (Figure 1D). To determine optimal OATP1B3 expression, the stable inducible LNCaP-OATP1B3 cell line was treated with DOX in a dose-and time-dependent manner. Maximal gene expression (71-fold increase in SLCO1B3 expression) was established at 300ng/mL following 24 hours of treatment (Figure 1E). Immunoblot analysis of the protein with an anti-GFP antibody detected a band corresponding to the predicted size of GFP-OATP1B3 (Figure 1F). Transport studies were repeated in the LNCaP-OATP1B3 cell line and DOX treatment resulted in an increase in ^{3}H-testosterone (~1.6-fold, P=0.0027) and ^{3}H-methotrexate uptake (1.2-fold and 1.5-fold, $P \leq 0.0001$ Figure 1G–H).

Influence of OATP1B3 on in vivo testosterone pharmacokinetics

To assess whether the *in vivo* disposition of testosterone was affected by OATP1B3, we measured its concentration in plasma and liver. ^{3}H-Testosterone was administered to male *Slco1b2*-knockout (KO) and male *Slco1b2*-knockout/*hSLCO1B3*-knock-in (KO/KI) mice. Liver AUC in KO/KI mice was 15% greater (1317 hr*nmol/L) than in KO (1150 hr*nmol/L, P=0.0040; Figure 2A). Consistent with lower liver exposure, KO mice also had a 17% greater plasma exposure (112 hr*nmol/L) than KO/KI mice (96hr*nmol/L, P=0.0030; Figure 2B). These results suggest that testosterone can be transported by the transgenic human OATP1B3 transporter *in vivo* and that testosterone disposition is influenced by the presence of OATP1B3 in the liver.

SLCO1B3 expression and regulation in prostate cancer cell lines

To further characterize the function of OATP1B3 and its potential role in mediating resistance to androgen deprivation in prostate cancer, we first determined the endogenous expression of all transporter systems in the commonly used *in vitro* cell line models (LNCaP, 22Rv1, PC3, and DU145) for CRPC versus androgen responsive prostate cancer. We used the TLDA, a medium throughput Taqman-based qRT-PCR assay, to evaluate the expression of 380 multidrug resistance (MDR)-related genes, involved in either intrinsic or acquired MDR, that were selected based on literature published over the past 30 years (17). The results show that OATP1B3 was the second most differentially expressed transporter in prostate cancer cells (116-fold greater in CRPC; Figure 3A). Androgen responsive prostate cell lines typically had greater expression of lt-SLCO1B3 whereas ct-SLCO1B3 was expressed at very high levels in most CRPC cell lines (Figure S2). Interestingly, the LNCaP-derived neuroendocrine CRPC cell line had very low expression of both isoforms, possibly due to high expression of the *SLCO1B3* repressor, FOXA2 (HNF3B) (Figure S2) (18,19).

Recent studies revealed that liver-specific OATP1B3 (hereafter referred to as the liver-type OATP1B3, or *lt-SLCO1B3*) exists in more than one isoform, and a cancer-type mRNA isoform of *SLCO1B3* (*ct-SLCO1B3*) has recently been identified in tumor cells (20,21). Hypoxia and hypoxia-inducible factor-1alpha (HIF-1α) have previously been shown to regulate the expression ct-SLCO1B3 (22), as several hypoxia response elements (HREs) are present in the gene (Figure S2). We next assessed which *SLCO1B3* isoform is specifically expressed in our prostate cancer cell models and whether hypoxia regulates its expression by

using $CoCl_2$, a hypoxia mimetic agent, to stimulate endogenous expression. Our immunohistochemistry (IHC) data showed that HIF-1α and OATP1B3 expression co-localize in prostate tumors (Figure S2); however, HIF-1α stabilization with $CoCl_2$ only slightly increased *lt-SLCO1B3* relative gene expression (RGE=100,000*$2^{-\Delta Ct}$) in LNCaP (median RGE=4.7 vs. median RGE =10.3, P=0.030) and DU145 cells (1.2 vs. 2.8, P=0.012), but did not affect *lt-SLCO1B3* expression in 22Rv1 (3.4 vs. 4.9, P=0.25) and PC3 cells (4.8 vs. 2.7, P=0.089; Figure S2). Cancer type *SLCO1B3* was only altered by $CoCl_2$ in 22Rv1 cells (Figure S2). Furthermore, results from our electrophoretic mobility shift assays in prostate cancer cells indicate that HIF-1α bound to certain HREs in *SLCO1B3* (Figure S2).

During our investigation of the hypoxic regulation of *SLCO1B3*, we unexpectedly discovered that chetomin, an inhibitor of the HIF-1α-p300 interaction, was a potent inducer of *SLCO1B3* transcripts. Chetomin robustly increased the expression of *lt-SLCO1B3* by ≥ 11.7-fold in each cell line (RGE=51.5, 451.5, 51.4, 19.2, respectively). Using primers that bind to either the exon 10–11 junction, the exon 3–4 junction, or the exon 1*-4 junction (Figure 3B), we determined RGE from qPCR data of total SLCO1B3 (t-SLCO1B3), *lt-SLCO1B3,* or *ct-SLCO1B3* in prostate cancer cell lines: LNCaP and 22Rv1 (Figure 3C–E). The prostate tumor cell lines (LNCaP, 22Rv1, PC3, and DU145) express *lt*-SLCO1B3 (median RGE=4.7, 5.1, 4.8, and 1.2, respectively). Basal expression of *ct-SLCO1B3* was greater in CRPC cell lines (median RGE=1870 and 1478, respectively) than in androgen-responsive cell lines (median RGE=1.1 and 5.8). Chetomin also increased *ct-SLCO1B3* expression by ≥21.2 fold in androgen-responsive cell lines (median RGE=22.4 and 394.5, respectively); however, it did not significantly change *ct-SLCO1B3* expression in PC3s, and it decreased *ct-SLCO1B3* expression in DU145s (RGE=798.9). *ct-SLCO1B3* expression in untreated LNCaP cells was also below the lower limit of quantification (LLoQ) in 4 of 8 assays (RGE=1).

Testosterone uptake following induction of endogenous SLCO1B3 expression

Since chetomin induces expression of endogenous *lt-SLCO1B3*, we next tested the hypothesis that increasing chetomin treatment time results in increased testosterone uptake in tumor cells. Chetomin-induced *SLCO1B3* expression was maximal at 48 hours of treatment in LNCaP cells (Figure 4A). Chetomin exposure time co-varied with testosterone uptake in cells incubated with ^{3}H-testosterone for 30 and 60 minutes (P≤0.020), and the slope of ^{3}H-testosterone uptake versus chetomin exposure time was significantly greater than zero in cells exposed to ^{3}H-testosterone for 60 versus 5 min (P=0.0042; Figure 4B). The steady-state intracellular testosterone concentration was approximately 2-fold higher in LNCaP cells treated with chetomin for 48 hours and incubated with ^{3}H-Testosterone for 60 minutes (P=0.042; Figure 4C) and approximately 1.5-fold higher in 22Rv1 cells (P=0.016; Figure 4D). Similar results were seen with another OATP1B3 substrate, methotrexate (P<0.0001; Figure 4E). Ursolic acid also inhibited testosterone uptake in both untreated and chetomin-treated cells (P≤0.043; Figure 4F).

Since *ct-SLCO1B3* is reported to have much-reduced transport activity (21), and CRPC cell lines express ≥234-fold greater levels of this isoform (mean RGE_{PC3}=854, RGE_{DU145}=1118) than *lt-SLCO1B3* (RGE_{PC3}=3.65 and RGE_{DU145}=1.21; Figure 3E), we

next tested whether siRNA knockdown of both isoforms of *SLCO1B3* (or total *SLCO1B3*, *t-SLCO1B3*) in DU145 and PC3 cells could result in decreased testosterone uptake. Two siRNAs were selected that reduced expression of both *lt-SLCO1B3* and *ct-SLCO1B3* by ≥63% in DU145 cells, which express very low levels of *lt-SLCO1B3* and very high levels of *ct-SLCO1B3* (*siSLCO1B3-1* and *siSLCO1B3-6*; Figure 4G). No differences in testosterone uptake were seen between cells treated with *siSLCO1B3-1* or *siSLCO1B3-6* or *si-control* (Figure 4H). These results were confirmed in PC3 cells (Figure S3).

Clinical relevance of SLCO1B3 expression in human prostate cancer tissues

Normal liver and normal testicle were the only tissues in which *lt-SLCO1B3* was observed in all samples (100%). Prostate cancer was the only tumor type that significantly expressed *lt-SLCO1B3 de novo* (observed in 12/21 patients, 57.1%) versus normal prostate tissue (observed in 0/5 patients, 0%, $P<0.043$; Figure 5A). Relative gene expression in prostate cancer was lower in magnitude than that of normal liver (median RGE=140 vs. median RGE= 185,000; Figure 5B); however, *lt-SLCO1B3* expression was higher than *ct-SLCO1B3* expression by >325-fold in prostate tissues (Figure S4). In normal testes, *ct-SLCO1B3* expression exceeded *lt-SLCO1B3* expression, but testicular tumors overexpressed *lt-SLCO1B3* (Figure S4). Of the tissue types studied, only the liver and testes express *lt-SLCO1B3* under normal conditions, while all other tissue types primarily expressed *ct-SLCO1B3.* Only in prostate tissue is there a statistically significant switch from primarily *ct-SLCO1B3* expression in normal tissue to *lt-SLCO1B3* expression in tumor tissue (Figure S4).

DISCUSSION

Although 75 years have passed since Huggins and Hodges discovered the role of androgens in prostate cancer (23), the translational relevance of their research remains prominent today: alluding to persistent androgen signaling from low levels of androgens produced in extragonadal sources, implicating this molecular pathway in the malignant phenotype of the disease, and speculating on mechanisms of treatment resistance (24). In the current era of molecularly targeted therapy, the arsenal of agents for prostate cancer treatment now includes androgen biosynthesis inhibitors (e.g., abiraterone) and AR antagonists (e.g., enzalutamide). While these drugs prolong survival in men with CRPC, they are not curative and resistance eventually develops (25). Therefore, it is critical to understand the mechanisms of resistance to androgen deprivation.

In this study, we showed that OATP1B3 is a functional transporter in prostate cancer cells. Testosterone is not only subject to simple diffusion across biological barriers (26) but also transported and concentrated inside prostate tumor tissues that overexpress OATP1B3 at the plasma membrane, affecting overall testosterone disposition and local testosterone concentrations alike. We also showed, for the first time, that hepatic hOATP1B3 can modulate the pharmacokinetics of testosterone *in vivo*.

Within prostate cancer cell lines, inducing endogenous OATP1B3 by chetomin or overexpression with a DOX-inducible OATP1B3 expression system was sufficient to increase intracellular testosterone by approximately 2-fold. However, only *lt-SLCO1B3*

appeared to be responsible for such increases since *ct-SLCO1B3* knockdowns did not affect intracellular testosterone concentrations, which was expected given that ct-OATP1B3 is neither extensively plasma-membrane-bound nor does it significantly increase substrate transport (21). Therefore, the biological consequences of *ct-SLCO1B3* expression are still unclear and its potential as a cancer-specific biomarker remains to be elucidated. Expression of *lt-SLCO1B3* still appears to result in increased testosterone uptake. This finding may explain why men with allelic variants that increase testosterone uptake efficiency have both a poorer prognosis (6,7,27), and a poorer response to androgen deprivation therapy (7,28).

It is currently unclear by which mechanism prostate tumor cells develop *de novo lt-SLCO1B3* expression. Previous studies on regulatory mechanisms for *SLCO1B3* expression have included the involvement of the liver-enriched transcription factor hepatocyte nuclear factor 3β (19), DNA methylation (29,30), and hypoxia-dependence (22) that varies depending on tissues types. In our study, HIF-1α stabilization by $CoCl_2$ only modestly increased *SLCO1B3* expression in prostate cancer cells. Our data suggest that HIF-1α-dependent induction is cell-type dependent and may rely on specific co-activators, particularly other transcription factors that may bind *cis*-regulatory regions around the active hypoxia response elements in the gene region surrounding the promoter of *lt-* and *ct-SLCO1B3* as well as protein-protein interactions that mediate specific activity of a particular isoform.

However, chetomin significantly increases the expression of both isoforms, which suggests that *SLCO1B3* expression is repressed by a p300-mediated mechanism. Interestingly, the *SLCO1B3* promoter contains p300 binding sites that are near the transcription start site, which complex with known *SLCO1B3* regulatory elements (i.e., FOXA1 and FOXA2) (19). Studies are currently underway to identify cofactors involved in forming the p300 transcriptional complex regulating *SLCO1B3* expression.

We demonstrated that six of nine transporters with >10-fold higher expression in CRPC represent isoforms that are known to affect the disposition of sterols (i.e., CMOAT2, OATP1B3, ABCA1, OATPE, ABCG4, and ABCA8 (31)) or are highly expressed in testicular tissues (OATP1B3, SLC34A2, and ABCA8; (8,32,33)). Of all extra-hepatic tissues evaluated, normal testicle and prostate tumors are the only tissues that frequently express *lt-SLCO1B3* at high levels. However, while some studies have evaluated *de novo t-SLCO1B3* expression in prostate tumors (6,8), the present study is the first to ascertain *lt-SLCO1B3* expression.

In summary, several previous studies have demonstrated that OATP1B3 expression is an important predictive and/or prognostic marker in men with prostate cancer (6,7,27,28). The present study clarifies that such differences in clinical outcome are likely attributed to differential steroid-hormone uptake in prostate tumor cells. Taken together, these results suggest that OATP1B3 is a major physiologic contributor to androgen disposition in man. OATP1B3 is clinically expressed and its *de novo* expression, particularly that of *lt-SLCO1B3*, contributes to the mechanism by which prostate tumors subvert physiologic androgen regulation (10). OATP1B3 should be considered a viable biological target for therapeutic intervention in prostate cancer.

Supplementary Material

Refer to Web version on PubMed Central for supplementary material.

Acknowledgments

Financial support: This study was supported in part by the Intramural Research Program of the National Institutes of Health, National Cancer Institute, Bethesda, MD, US.

References

1. Pienta KJ, Bradley D. Mechanisms underlying the development of androgen-independent prostate cancer. Clin Cancer Res. 2006; 12(6):1665–71. DOI: 10.1158/1078-0432.CCR-06-0067 [PubMed: 16551847]
2. Scher HI, Sawyers CL. Biology of progressive, castration-resistant prostate cancer: directed therapies targeting the androgen-receptor signaling axis. J Clin Oncol. 2005; 23(32):8253–61. DOI: 10.1200/JCO.2005.03.4777 [PubMed: 16278481]
3. Mostaghel EA, Page ST, Lin DW, Fazli L, Coleman IM, True LD, et al. Intraprostatic androgens and androgen-regulated gene expression persist after testosterone suppression: therapeutic implications for castration-resistant prostate cancer. Cancer Res. 2007; 67(10):5033–41. DOI: 10.1158/0008-5472.CAN-06-3332 [PubMed: 17510436]
4. Montgomery RB, Mostaghel EA, Vessella R, Hess DL, Kalhorn TF, Higano CS, et al. Maintenance of intratumoral androgens in metastatic prostate cancer: a mechanism for castration-resistant tumor growth. Cancer Res. 2008; 68(11):4447–54. DOI: 10.1158/0008-5472.CAN-08-0249 [PubMed: 18519708]
5. Giorgi EP. Studies on androgen transport into canine prostate in vitro. The Journal of endocrinology. 1976; 68(1):109–19. [PubMed: 943457]
6. Wright JL, Kwon EM, Ostrander EA, Montgomery RB, Lin DW, Vessella R, et al. Expression of SLCO transport genes in castration-resistant prostate cancer and impact of genetic variation in SLCO1B3 and SLCO2B1 on prostate cancer outcomes. Cancer Epidemiol Biomarkers Prev. 2011; 20(4):619–27. DOI: 10.1158/1055-9965.EPI-10-1023 [PubMed: 21266523]
7. Yang M, Xie W, Mostaghel E, Nakabayashi M, Werner L, Sun T, et al. SLCO2B1 and SLCO1B3 may determine time to progression for patients receiving androgen deprivation therapy for prostate cancer. J Clin Oncol. 2011; 29(18):2565–73. DOI: 10.1200/JCO.2010.31.2405 [PubMed: 21606417]
8. Pressler H, Sissung TM, Venzon D, Price DK, Figg WD. Expression of OATP family members in hormone-related cancers: potential markers of progression. PloS one. 2011; 6(5):e20372.doi: 10.1371/journal.pone.0020372 [PubMed: 21625523]
9. Shitara Y, Maeda K, Ikejiri K, Yoshida K, Horie T, Sugiyama Y. Clinical significance of organic anion transporting polypeptides (OATPs) in drug disposition: their roles in hepatic clearance and intestinal absorption. Biopharmaceutics & drug disposition. 2013; 34(1):45–78. DOI: 10.1002/bdd.1823 [PubMed: 23115084]
10. Sissung TM, Reece KM, Spencer S, Figg WD. Contribution of the OATP1B subfamily to cancer biology and treatment. Clinical pharmacology and therapeutics. 2012; 92(5):658–60. DOI: 10.1038/clpt.2012.127 [PubMed: 23010650]
11. Gui C, Miao Y, Thompson L, Wahlgren B, Mock M, Stieger B, et al. Effect of pregnane X receptor ligands on transport mediated by human OATP1B1 and OATP1B3. European journal of pharmacology. 2008; 584(1):57–65. DOI: 10.1016/j.ejphar.2008.01.042 [PubMed: 18321482]
12. Treiber A, Schneiter R, Hausler S, Stieger B. Bosentan is a substrate of human OATP1B1 and OATP1B3: inhibition of hepatic uptake as the common mechanism of its interactions with cyclosporin A, rifampicin, and sildenafil. Drug metabolism and disposition: the biological fate of chemicals. 2007; 35(8):1400–7. DOI: 10.1124/dmd.106.013615 [PubMed: 17496208]

13. Carver J, Dexheimer TS, Hsu D, Weng MT, Smith JL, Guha R, et al. A high-throughput assay for small molecule destabilizers of the KRAS oncoprotein. PloS one. 2014; 9(8):e103836.doi: 10.1371/journal.pone.0103836 [PubMed: 25093678]

14. Bailer AJ. Testing for the equality of area under the curves when using destructive measurement techniques. J Pharmacokinet Biopharm. 1988; 16(3):303–9. [PubMed: 3221328]

15. Chang KH, Li R, Papari-Zareei M, Watumull L, Zhao YD, Auchus RJ, et al. Dihydrotestosterone synthesis bypasses testosterone to drive castration-resistant prostate cancer. Proceedings of the National Academy of Sciences of the United States of America. 2011; 108(33):13728–33. DOI: 10.1073/pnas.1107898108 [PubMed: 21795608]

16. Gui C, Obaidat A, Chaguturu R, Hagenbuch B. Development of a cell-based high-throughput assay to screen for inhibitors of organic anion transporting polypeptides 1B1 and 1B3. Current chemical genomics. 2010; 4:1–8. DOI: 10.2174/1875397301004010001 [PubMed: 20448812]

17. Calcagno AM, Salcido CD, Gillet JP, Wu CP, Fostel JM, Mumau MD, et al. Prolonged drug selection of breast cancer cells and enrichment of cancer stem cell characteristics. J Natl Cancer Inst. 2010; 102(21):1637–52. DOI: 10.1093/jnci/djq361 [PubMed: 20935265]

18. Qi J, Nakayama K, Cardiff RD, Borowsky AD, Kaul K, Williams R, et al. Siah2-dependent concerted activity of HIF and FoxA2 regulates formation of neuroendocrine phenotype and neuroendocrine prostate tumors. Cancer Cell. 2010; 18(1):23–38. DOI: 10.1016/j.ccr.2010.05.024 [PubMed: 20609350]

19. Vavricka SR, Jung D, Fried M, Grutzner U, Meier PJ, Kullak-Ublick GA. The human organic anion transporting polypeptide 8 (SLCO1B3) gene is transcriptionally repressed by hepatocyte nuclear factor 3beta in hepatocellular carcinoma. J Hepatol. 2004; 40(2):212–8. [PubMed: 14739090]

20. Nagai M, Furihata T, Matsumoto S, Ishii S, Motohashi S, Yoshino I, et al. Identification of a new organic anion transporting polypeptide 1B3 mRNA isoform primarily expressed in human cancerous tissues and cells. Biochemical and biophysical research communications. 2012; 418(4): 818–23. DOI: 10.1016/j.bbrc.2012.01.115 [PubMed: 22326869]

21. Thakkar N, Kim K, Jang ER, Han S, Kim K, Kim D, et al. A cancer-specific variant of the SLCO1B3 gene encodes a novel human organic anion transporting polypeptide 1B3 (OATP1B3) localized mainly in the cytoplasm of colon and pancreatic cancer cells. Molecular pharmaceutics. 2013; 10(1):406–16. DOI: 10.1021/mp3005353 [PubMed: 23215050]

22. Han S, Kim K, Thakkar N, Kim D, Lee W. Role of hypoxia inducible factor-1alpha in the regulation of the cancer-specific variant of organic anion transporting polypeptide 1B3 (OATP1B3), in colon and pancreatic cancer. Biochemical pharmacology. 2013; 86(6):816–23. DOI: 10.1016/j.bcp.2013.07.020 [PubMed: 23924606]

23. Huggins C, Hodges CV. Studies on prostatic cancer. I. The effect of castration, of estrogen and of androgen injection on serum phosphatases in metastatic carcinoma of the prostate. Cancer Res. 1941; 1:293–7.

24. Nelson WG. Commentary on Huggins and Hodges: “Studies on Prostatic Cancer”. Cancer Res. 2016; 76(2):186–7. DOI: 10.1158/0008-5472.CAN-15-3172 [PubMed: 26773095]

25. Antonarakis ES. Current understanding of resistance to abiraterone and enzalutamide in advanced prostate cancer. Clin Adv Hematol Oncol. 2016; 14(5):316–9. [PubMed: 27379691]

26. Setchell BP, Laurie MS, Main SJ, Goats GC. Mechanism of Transport of Testosterone through Walls of Seminiferous Tubules of Rat Testis. Int J Androl. 1978:506–12.

27. Hamada A, Sissung T, Price DK, Danesi R, Chau CH, Sharifi N, et al. Effect of SLCO1B3 haplotype on testosterone transport and clinical outcome in caucasian patients with androgen-independent prostatic cancer. Clin Cancer Res. 2008; 14(11):3312–8. DOI: 10.1158/1078-0432.CCR-07-4118 [PubMed: 18519758]

28. Sharifi N, Hamada A, Sissung T, Danesi R, Venzon D, Baum C, et al. A polymorphism in a transporter of testosterone is a determinant of androgen independence in prostate cancer. BJU Int. 2008; 102(5):617–21. DOI: 10.1111/j.1464-410X.2008.07629.x [PubMed: 18537956]

29. Ichihara S, Kikuchi R, Kusuhara H, Imai S, Maeda K, Sugiyama Y. DNA methylation profiles of organic anion transporting polypeptide 1B3 in cancer cell lines. Pharm Res. 2010; 27(3):510–6. DOI: 10.1007/s11095-010-0064-3 [PubMed: 20130966]

30. Imai S, Kikuchi R, Tsuruya Y, Naoi S, Nishida S, Kusuhara H, et al. Epigenetic regulation of organic anion transporting polypeptide 1B3 in cancer cell lines. Pharm Res. 2013; 30(11):2880–90. DOI: 10.1007/s11095-013-1117-1 [PubMed: 23812637]

31. Klaassen CD, Aleksunes LM. Xenobiotic, bile acid, and cholesterol transporters: function and regulation. Pharmacol Rev. 2010; 62(1):1–96. DOI: 10.1124/pr.109.002014 [PubMed: 20103563]

32. Corut A, Senyigit A, Ugur SA, Altin S, Ozcelik U, Calisir H, et al. Mutations in SLC34A2 cause pulmonary alveolar microlithiasis and are possibly associated with testicular microlithiasis. Am J Hum Genet. 2006; 79(4):650–6. DOI: 10.1086/508263 [PubMed: 16960801]

33. Ohtsuki S, Kamoi M, Watanabe Y, Suzuki H, Hori S, Terasaki T. Correlation of induction of ATP binding cassette transporter A5 (ABCA5) and ABCB1 mRNAs with differentiation state of human colon tumor. Biol Pharm Bull. 2007; 30(6):1144–6. [PubMed: 17541169]

Implications

The present study suggests that de novo OATP1B3 expression in prostate cancer drives greater androgen uptake and is consistent with previous observations that greater OATP1B3 activity results in the development of Androgen Deprivation Therapy resistance and shorter overall survival.

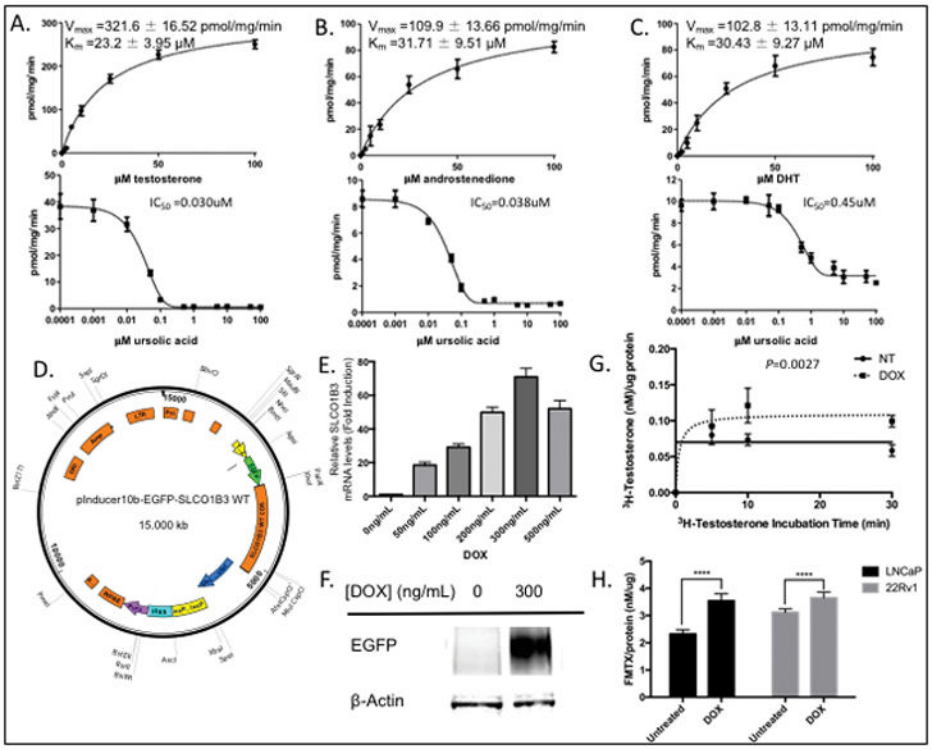

FIGURE 1.

Michaelis-Menten plots of androgens −/+ ursolic acid: (A) [^{3}H]-testosterone, (B) [^{3}H]-4-androstan-3,17-dione (androstenedione), and (C) [^{3}H]-5-androstan-17-ol-3-one (DHT) uptake in OATP1B3-expressing CHO cells. Results are expressed as mean + SD of triplicate determinations from three independently performed experiments. To ascertain whether lt-OATP1B3 promoted cellular uptake of testosterone, (D) a doxycycline-inducible EGFP-linked SLCO1B3 lentiviral vector was designed and infected into LNCaP cells, and (E) the optimal doxycycline dose was found to be 300ng/mL, which (F) increased protein expression of GFP-labeled OATP1B3. Cells expressing this construct demonstrated a greater steady-state intracellular (G) [^{3}H]-testosterone and (H) [^{3}H]-methotrexate concentration ($P \leq 0.0001$). All included experiments include ≥3 biological and ≥3 technical replicates. ****P<0.0001.

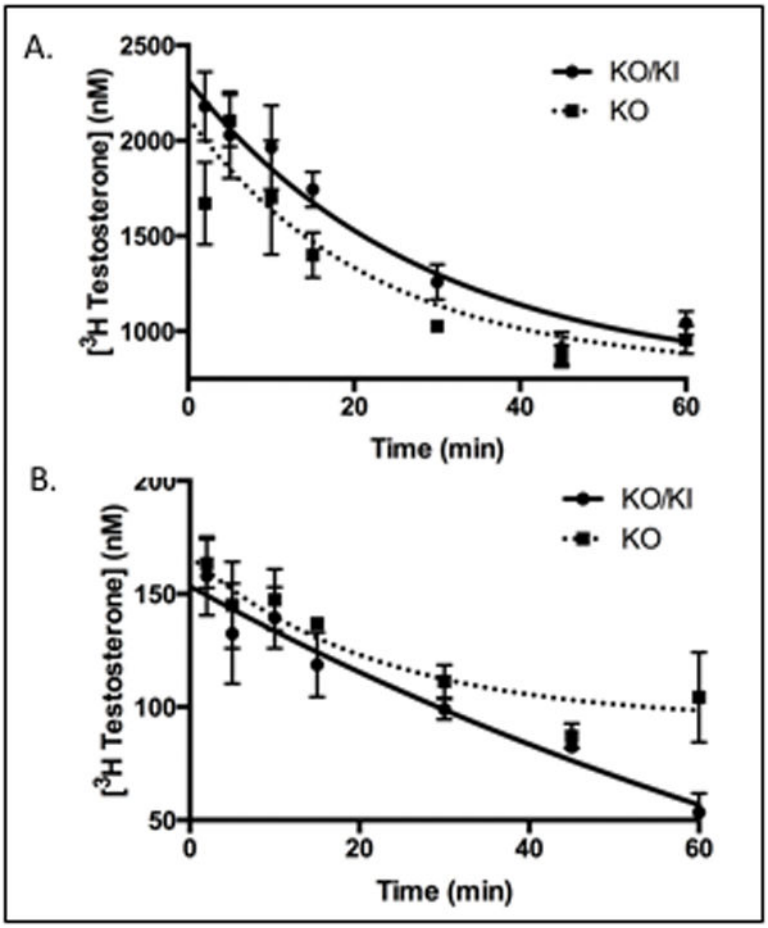

FIGURE 2.

The *in vivo* disposition of ^{3}H-testosterone was different in *Slco2b1*-knockout (KO) and male *Slco1b2*-knockout/*hSLCO1B3*-knock-in (KO/KI) mice. (A) Liver AUC in KO/KI mice was 15% greater (1317 hr*nmol/L) than in KO (1150 hr*nmol/L, P=0.0040). (B) KO mice also had a 17% greater plasma exposure (112 hr*nmol/L) than KO/KI mice (96hr*nmol/L, P=0.0030). All included experiments include ≥3 biological and ≥3 technical replicates. P-values were calculated using Bailer's method.

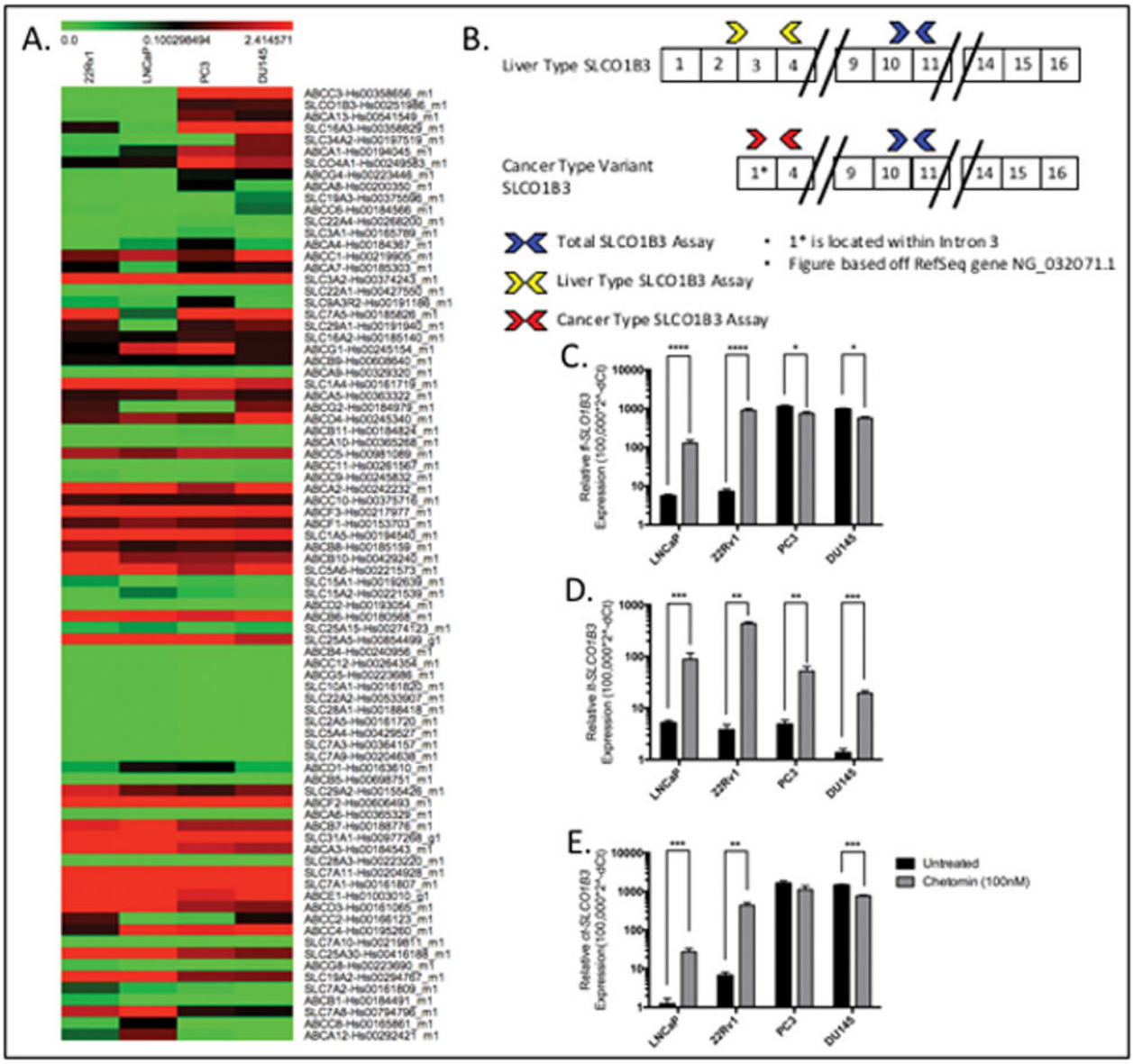

FIGURE 3.

OATP1B3 was (A) the second most differentially expressed transporter in hormone sensitive versus castration resistant prostate cancer cells (116-fold greater in CRPC) in a Taqman Low Density Array (TLDA). Primers that (B) distinguish between total-*SLCO1B3* (exon 10–11 border), liver type *SLCO1B3* (exon 3–4 border), and cancer type *SLCO1B3* (1*-4 border), and these primers were used to ascertain *SLCO1B3* expression in each of the prostate tumor cell lines in vehicle-control and chetomin-treated cells. Chetomin increased expression of (C) *t-SLCO1B3* in hormone sensitive cell lines while it decreased expression in CRPC. In all cell lines (D) *lt-SLCO1B3* expression was increased by chetomin treatment while (E) *ct-SLCO1B3* expression reflected similar changes to *t-SLCO1B3* (except in PC3 cells). All included experiments include ≥3 biological and ≥3 technical replicates.

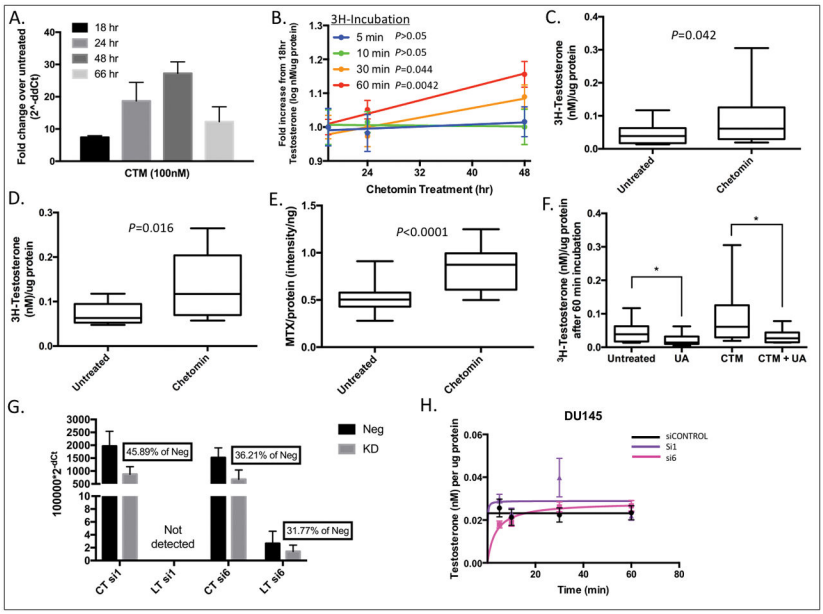

FIGURE 4.

SLCO1B3 expression became progressively higher between (A) 18, 24, and 48 hours in LNCaP cells treated with chetomin (100nM). Testosterone uptake was evaluated in (B) LNCaP cells following treatment with chetomin for 18, 24, and 48 hours and [^{3}H]-testosterone incubation times ranging from 5 to 60 minutes, and sixty minutes of incubation led to a significantly positive slope of the lines vs. that of 5 minutes (P=0.0042). Testosterone uptake was significantly greater in (C) LNCaP cells (*P*=0.042) and (D) 22Rv1 cells (*P*=0.016) that were pretreated with chetomin (100nM, 48hr) vs. untreated controls and (E) methotrexate uptake was also greater in chetomin-treated 22Rv1 cells (*P*<0.0001). The specific OATP1B3 inhibitor, ursolic acid (350nM), (F) inhibited testosterone uptake in LNCaP cells that were either untreated or exposed to chetomin. Finally, (G) *lt-SLCO1B3* and *ct-SLCO1B3* expression were evaluated in DU145 cells treated with *SLCO1B3*-specific siRNA (si1, and/or si6), and siRNA treated (H) DU145 cells did not demonstrate a decrease in testosterone uptake. All included experiments include ≥3 biological and ≥3 technical replicates. **P*<0.05, ****P*<0.001.

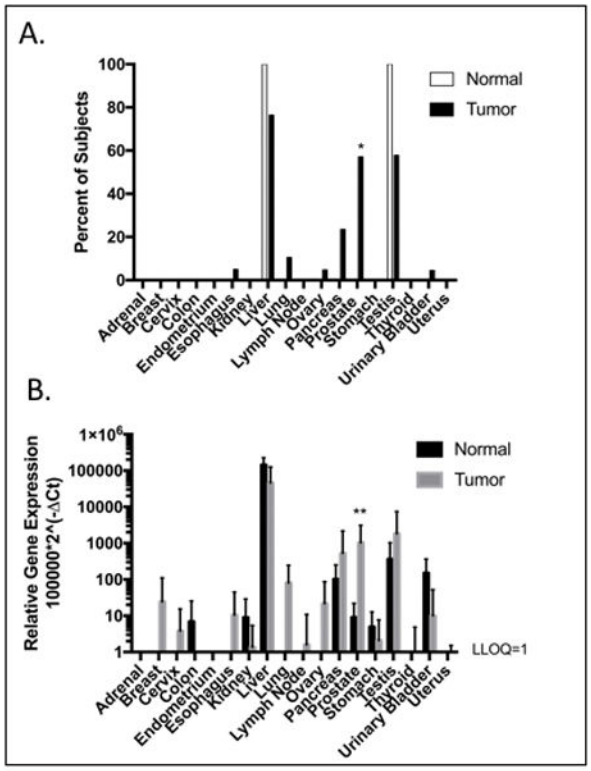

FIGURE 5.

The (A) percent of 384 normal and tumor tissue samples expressing *lt-SLCO1B3* and (B) the mean (+SD) of *lt-SLCO1B3* expression in the same 384 normal and tumor tissue samples was ascertained. Primary prostate cancer was the only example in which the magnitude of *lt-SLCO1B3* was significantly upregulated in tumor cells versus normal. **P*<0.05, **P<0.01. Sample availability limited number of replicates to 1 biological and 1 technical replicate per lt, ct, and full length *SLCO1B3* qPCR experiment.